NRIAG Journal of Astronomy and Geophysics 7 (2018) 99–106

Contents lists available at ScienceDirect

NRIAG Journal of Astronomy and Geophysics

journal homepage: www.elsevier.com/locate/nrjag

Full length article

Geophysical characterization of the role of fault and fracture systems for recharging groundwater aquifers from surface water of Lake Nasser

Khamis Mansour[a,*], Khaled Omar[a], Kamal Ali[b], Mohamed Abdel Zaher[a]

[a] National Research Institute of Astronomy and Geophysics, Helwan, Egypt
[b] Research Institute for Groundwater, National Water Research Center, Egypt

ARTICLE INFO

Keywords:
Fracture system
Seismicity
Groundwater reservoir
Gravity
VES

ABSTRACT

The role of the fracture system is important for enhancing the recharge or discharge of fluids in the subsurface reservoir. The Lake Nasser is consider one of the largest artificial lakes all over the world and contains huge bulk of storage water. In this study, the influence of fracture zones on subsurface fluid flow in groundwater reservoirs is investigated using geophysical techniques including seismicity, geoelectric and gravity data. These data have been utilized for exploring structural structure in south west Lake Nasser, and subsurface discontinuities (joints or faults) notwithstanding its related fracture systems. Seismicity investigation gave us the comprehension of the dynamic geological structure sets and proposing the main recharging paths for the Nubian aquifer from Lake Nasser surface water. Processing and modelling of aerogravity data show that the greater thickness of sedimentary cover (700 m) is located eastward and northward while basement outcrops occur at Umm Shaghir and Al Asr areas. Sixty-nine vertical electrical soundings (VES's) were used to delineate the subsurface geoelectric layers along eight profiles that help to realize the subsurface geological structure behind the hydrogeological conditions of the studied area.

1. Introduction

In Egypt, The population is rapidly growing now exceeding 90 million and the majority lives in less than 6% of its land area. To overcome this, the government of Egypt has been implementedmany engineering projects in southwestern Egypt for the purpose of managing its water resources and expanding its agricultural areas (Taha et al., 2009). The High Dam of Aswan was constructed in the 1960s to store the flooded water which came from The Nile upstream. The building of the Aswan High Dam caused the creation of the second largestworld artificial lake called Lake Nasser, and caused continuous recharge of the underlying Nubian aquifer either due to natural infiltration process or through the fault systems, and the fracture systems located around that Lake (Khamis et al., 2014). The study area is suitable for the conjunctive management of groundwater and Nile water for sustainable development. It is located between latitudes 22°30′ and 23°00′N and longitudes 31°25′ and 31°50′E. It covers an area of about 2567 km^2 as shown in Fig. 1.

The groundwater flow and contaminant transport, are predominantly provided through an insufficient number of dominant fractures, consequently, the precise characterization of these fractures and fault zones, as well as their connectivity is of supreme importance in prognosticating the hydraulic behaviour. In this paper, we concern mainly with the contributions of the Lake Nasser for recharging subsurface aquifers and the role of geological structure of fault systems as well as accompanied fractures in this process. Integrated geophysical data including seismicity, gravity and geoelectric measurements were used for investigating tectonic structure in south west of the Lake, and subsurface discontinuities (joints or faults) in addition to its associated fracture systems. Moreover, analysis of seismicity map helps to understand the active geological structure sets and proposing the main recharging paths for the Nubian aquifer from Lake Nasser surface water (see Table 1).

2. Geological setting

Study area is considered as a part of the stable shelf that lies to the north western edge of the Nubian Shield. The earth surface is comprised of plain sand sheet; the altitude is from 280 m to 165 m above sea level.

This sand sheet is bounded from the north by a carbonate plateau of 500 m height above sea level and is bounded from the east by the Red Sea granitic mountains series that attain a height of 1000 above sea

Peer review under responsibility of National Research Institute of Astronomy and Geophysics.
* Corresponding author.
E-mail address: kham123@hotmail.com (K. Mansour).

https://doi.org/10.1016/j.nrjag.2018.02.001
Received 2 January 2018; Received in revised form 2 February 2018; Accepted 7 February 2018
Available online 23 February 2018

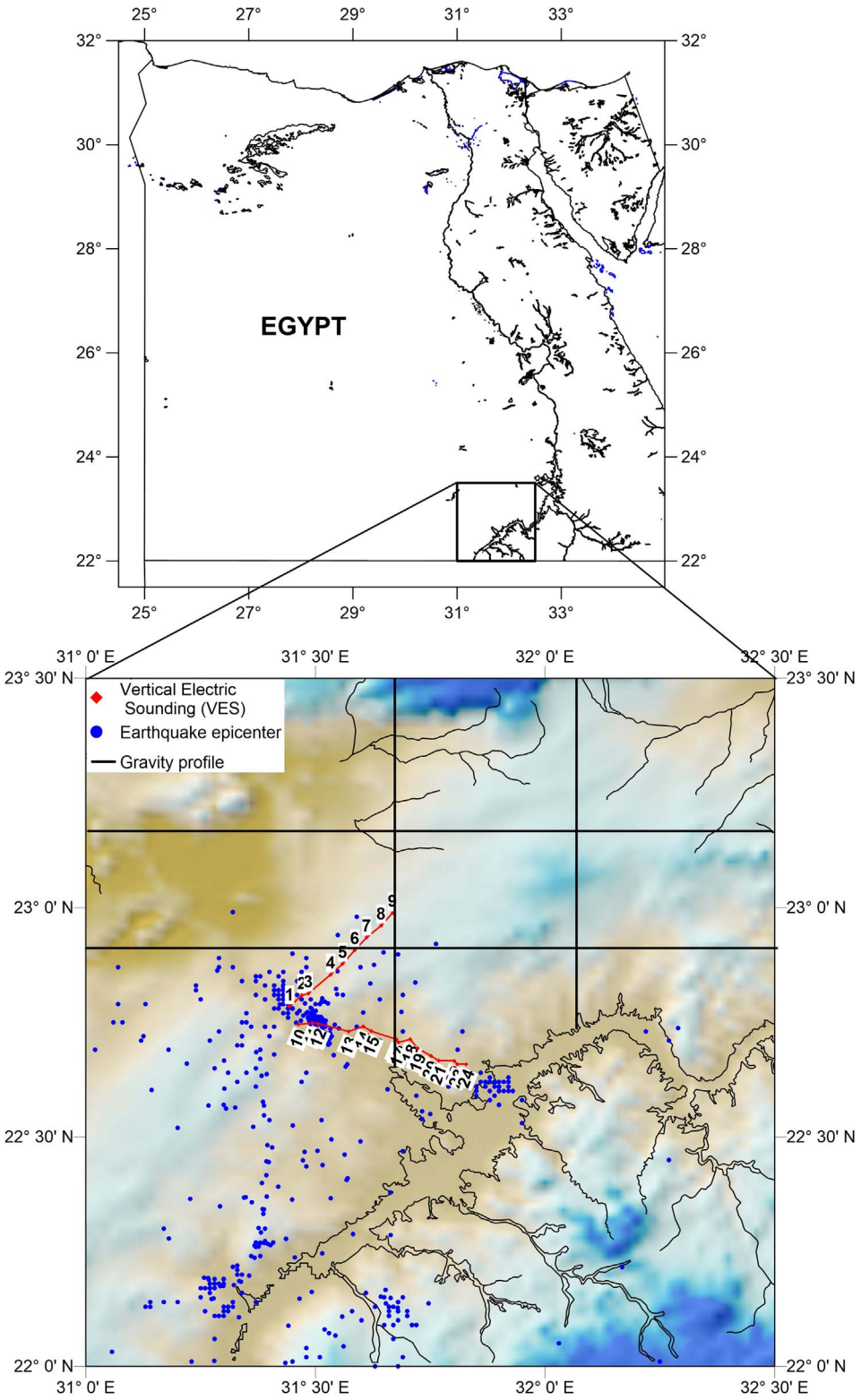

Fig. 1. Location map of Lake Nasser showing the distributions of earthquake epicentral (blue dotes), locations of VES measured stations (red squares) and gravity profiles used for 2D modeling (black lines).

level. The existence of this mountains series may explain the existence of the short wadies slope towards Toshka area from the east i.e. Wadi El Alaqi. The Naser Lake basin is bounded by a group of Khours, e.g. Toshka and Klabshakhours. There are some plains penetrate El Kharga Oasis depression and extend to the Toshka depression. From western side of these plains there is a thick belt of sand dunes about of 30 km, this belt extends to the north towards Baris Oasis, and to the north towards Salima Oasis in the north of Sudan. Fig. 2 shows the geological map of Lake Nasser area (CONOCO, 1987).

3. Seismicity around Lake Nasser

The earthquakes in the study area were collected for the period from 1982 to 2006 principally and gathered from Aswan seismic Bulletin,

Table 1
List of earthquake events in/around Lake Nasser, collected from Aswan, Abu–Simbil, Marsa Alam seismic stations, Aswan seismic network and Egyptian National Seismic Network during 1982–2014.

Year	Mon.	Day	Hr.	Min.	Sec.	Lat. (N)	Long. (E)	ML
2013	2	25	13	57	56.23	23.5343	32.4945	1.91
2013	2	25	13	57	56.23	23.5343	32.4945	1.91
2014	4	5	22	12	47.15	22.749	31.4581	1.37
2014	8	11	23	15	31.87	22.7597	31.4841	1.41
2014	7	11	1	34	56.48	22.7326	31.4902	1.46
2014	7	6	22	3	24.55	22.7016	31.5282	1.55
2014	5	2	11	16	34.7	22.758	31.5145	1.58
2014	8	11	23	19	19.18	22.7504	31.4921	1.6
2014	4	6	3	12	45.32	22.3012	31.376	1.72
2014	5	30	15	23	51.47	22.7556	31.509	1.9
2014	5	21	4	38	35.27	22.8755	31.6273	1.95
2014	3	15	7	29	7.09	22.343	31.385	1.98
2014	4	6	3	18	36.66	22.2917	31.3816	2
2014	5	27	5	33	42.94	22.3997	31.3836	2.07
2014	7	24	8	37	13.71	22.2371	31.455	2.11
2014	1	28	2	29	8.33	22.7196	31.5358	2.13
2014	3	19	21	3	49.06	22.7285	31.519	2.18
2014	4	7	13	49	16.74	22.3682	31.3442	2.22
2014	4	7	4	17	38.44	22.3486	31.2924	2.35
2014	3	6	20	58	47.04	22.3323	31.3863	2.38
2014	3	8	22	31	16.83	22.5217	31.3646	2.45
2014	5	22	3	36	50.3	22.3632	31.4493	2.46
2014	3	5	13	19	8.95	22.4166	31.3929	2.48
2014	7	27	19	12	40	22.8372	31.7175	2.48
2014	5	23	6	3	58.82	22.7512	31.5155	2.56
2014	3	5	14	23	6.45	22.3578	31.3617	2.58
2014	5	13	17	3	46.56	22.7194	31.1256	2.64
2014	5	24	14	48	49.52	22.4688	31.6904	2.64
2014	4	18	2	19	20.7	22.4467	31.3932	2.67
2014	4	26	21	1	45.24	22.3917	31.4193	2.69
2014	1	31	7	48	4.6	22.7543	31.4988	2.72
2014	3	25	18	40	8.31	22.4774	31.406	2.82
2014	3	4	22	30	53.31	22.6053	31.3019	2.84
2014	3	4	14	16	49.9	22.7502	31.4919	2.96
2014	5	13	17	3	46.56	22.7194	31.1256	2.64
2014	4	7	4	17	38.44	22.3486	31.2924	2.35
2014	3	4	22	30	53.31	22.6053	31.3019	2.84
2014	4	7	13	49	16.74	22.3682	31.3442	2.22
2014	3	5	14	23	6.45	22.3578	31.3617	2.58
2014	3	8	22	31	16.83	22.5217	31.3646	2.45
2014	4	6	3	12	45.32	22.3012	31.376	1.72
2014	4	6	3	18	36.66	22.2917	31.3816	2
2014	5	27	5	33	42.94	22.3997	31.3836	2.07
2014	3	15	7	29	7.09	22.343	31.385	1.98
2014	3	6	20	58	47.04	22.3323	31.3863	2.38
2014	3	5	13	19	8.95	22.4166	31.3929	2.48
2014	4	18	2	19	20.7	22.4467	31.3932	2.67
2014	3	25	18	40	8.31	22.4774	31.406	2.82
2014	4	26	21	1	45.24	22.3917	31.4193	2.69
2014	5	22	3	36	50.3	22.3632	31.4493	2.46
2014	7	24	8	37	13.71	22.2371	31.455	2.11
2014	4	5	22	12	47.15	22.749	31.4581	1.37
2014	8	11	23	15	31.87	22.7597	31.4841	1.41
2014	7	11	1	34	56.48	22.7326	31.4902	1.46
2014	3	4	14	16	49.9	22.7502	31.4919	2.96
2014	8	11	23	19	19.18	22.7504	31.4921	1.6
2014	1	31	7	48	4.6	22.7543	31.4988	2.72
2014	5	30	15	23	51.47	22.7556	31.509	1.9
2014	5	2	11	16	34.7	22.758	31.5145	1.58
2014	5	23	6	3	58.82	22.7512	31.5155	2.56
2014	3	19	21	3	49.06	22.7285	31.519	2.18
2014	7	6	22	3	24.55	22.7016	31.5282	1.55
2014	1	28	2	29	8.33	22.7196	31.5358	2.13
2014	5	21	4	38	35.27	22.8755	31.6273	1.95
2014	5	24	14	48	49.52	22.4688	31.6904	2.64
2014	7	27	19	12	40	22.8372	31.7175	2.48

ENSN (Egyptian National Seismological Network) and Aswan, Abu–Simbil, Marsa Alam seismic stations. The epicentral divisions of the recorded earthquakes in Tushka zone and its region are appeared in Fig. 3.

These events have magnitude range from 1 to 4. Some of these events are situated in the north-western part and westward of the Tushka New City site. Southward of Tushka zone events are situated in and around Abu Simbel City. In addition to the southeast Tushka region, some events with magnitudes range from 2.5 to 4 are situated in Allaqi zone (East southern corner of the Eastern Desert). The majority of these events are situated mainly in Wadi Allaqi (QabQaba zone) and they range in magnitudes from 2.5 to 3.8. On the other hand, events are situated between the East bank of Nasser Lake and Qabqaba zone. Two of these events have magnitude 3.0 and 4 are suitedin the north and southeast of Abu Simble City (about 40 km) on the Eastern side of Nasser Lake (Fig. 3).

Figs. 4 and 5 demonstrate the distribution of the depths of the foci of the earthquakes that took place in the area since January 1982 to September 2014. Plainly the profundities of earthquakesfocus from 5 to 25 km and the records of earthquakes focused in the North areas of the zone of study and abatements southward (Fig. 4). Then again, the records of seismic earthquakes focused in the two areas; Tushka in the south of the Nile and north and Abu Simbel (Fig. 5).

4. Aerogravity data

Airborne gravity anomaly maps scale 1:500,000 (1 mGal contour interval) was aggregated by the Egyptian General Petroleum Corporation (EGPC) (1980) and used for providing information about the internal structure of the Earth's crust in the area of study (Fig. 6a).

The study of the gravity data suggests the existence of closed anomalies of various shapes, patterns, and amplitudes. These anomalies can be explicated as the consequence of structures influencing the basement surface and inside the sedimentary cover. The examination of the investigation area's aerogravity map finds out that the Bouguer anomalies range from +3 to −35 mGal. Positive gravity anomaly is the most part because of elevate of denser basement rocks in El Asr and Umm shaghir, while, the lower gravity values suggest thick of sedimentary cover. The linear anomalies in the gravity map (NE-SW striking trend) might be because of fractures and faults influencing the basement surface, and expand upward into the sedimentary cover. Close anomalies of different amplitudes are observed in different parts of the area. These anomalies are represented by negative polarities of different values at the northern eastern parts and close to Lake Naser or positive at the central parts adjacent to Umm Shaghir and El Asr mountains.

The horizontal gradient separates gravity sources and recognizes contacts between the lithological units (Fig. 6c). The technique confirms that the horizontal gradient of the gravity anomaly created by a tabular body tends to overlie the edges of the body if the edges are vertical and well-separated (Cordell, 1979; Cordell and Grauch, 1985). It is based on the principle that a nearly vertical, fault-like boundary provides gravity anomaly whose horizontal gradient is highest directly above the top edge of the boundary (Grauch, 1987). Certainly, the superposition of the maxima-determined densities on different scales can highlight the several contacts present on the horizontal gradient map. The method also describes both deep and shallow sources more robustly than the vertical gradient method, which is helpful only in recognizing shallower structures.

The tilt gradient of the aerogravity map is displayed in Fig. 6d. The tilt gradient is the proportion of the vertical gradient over the total horizontal gradient of the gravity field. The tilt gradient intensifies small anomalies and brings up particular structural and lithological information. Linear features with a NE-SW striking trend are pronounced in the tilt gradient map. The processed maps show a good correction between the gravity anomalies and the structural lines and limestone escarpment in the geological map.

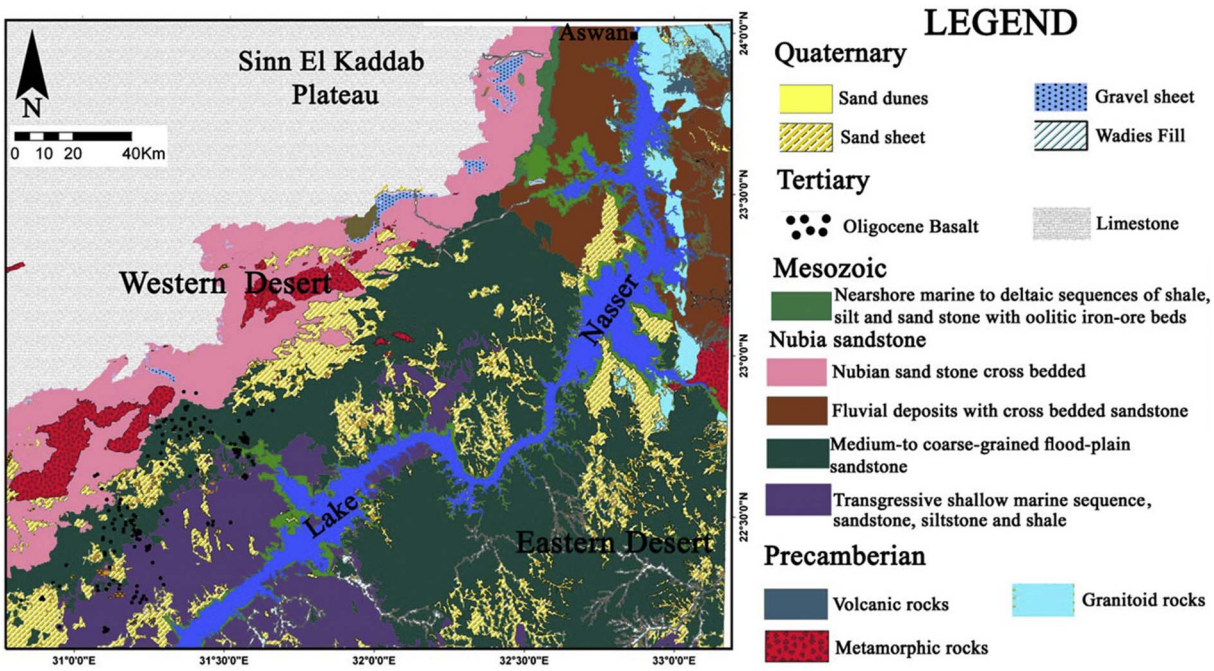

Fig. 2. The geologic map of the Lake Nasser area taken from CONOCO (1987).

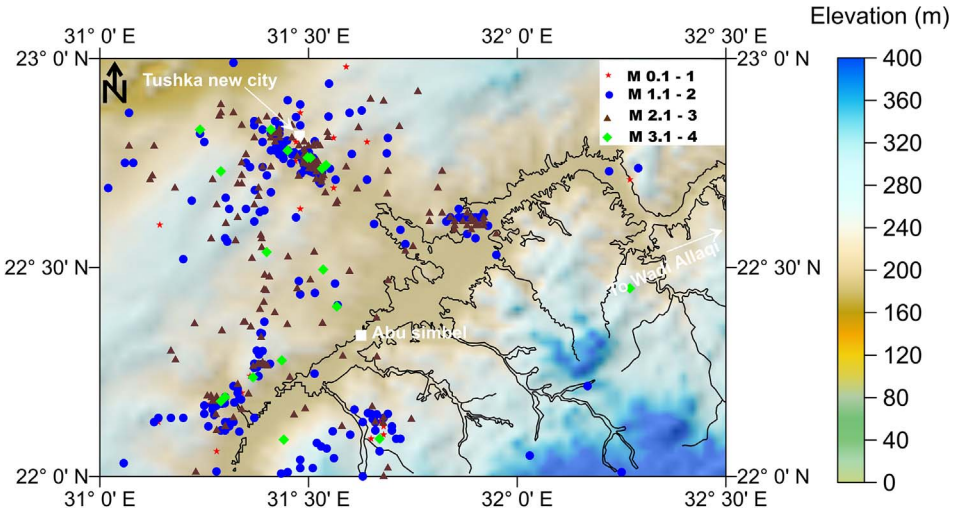

Fig. 3. Distribution of Earthquake epicentral in/and around the Tushka New City site dropped on a topographic map (DEM from a satellite dataset). These data were collected from Aswan, Abu–Simbil, Marsa Alam seismic stations, Aswan seismic network and Egyptian National Seismic Network during 1982 to 2014.

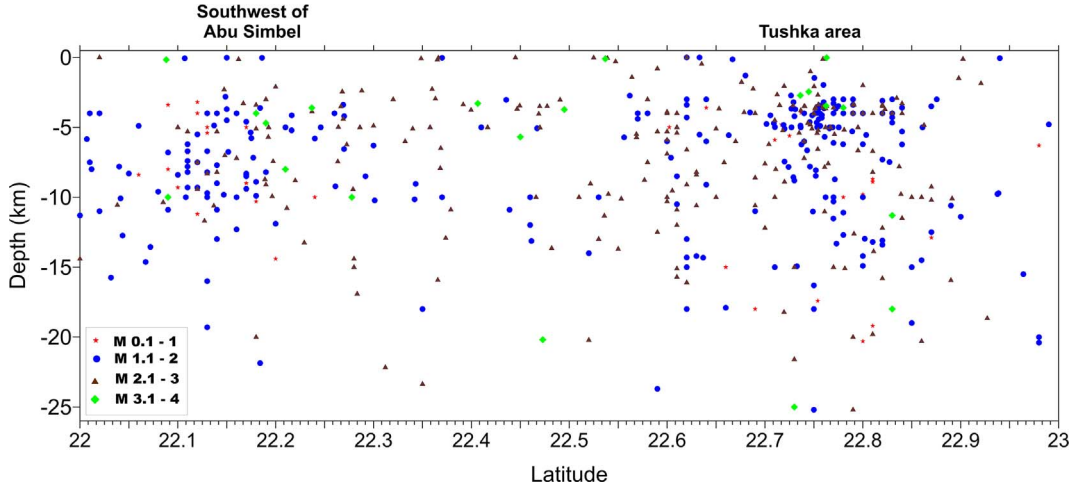

Fig. 4. Cross section shows distributions of earthquake events in south-north direction crossing Tushka New city area.

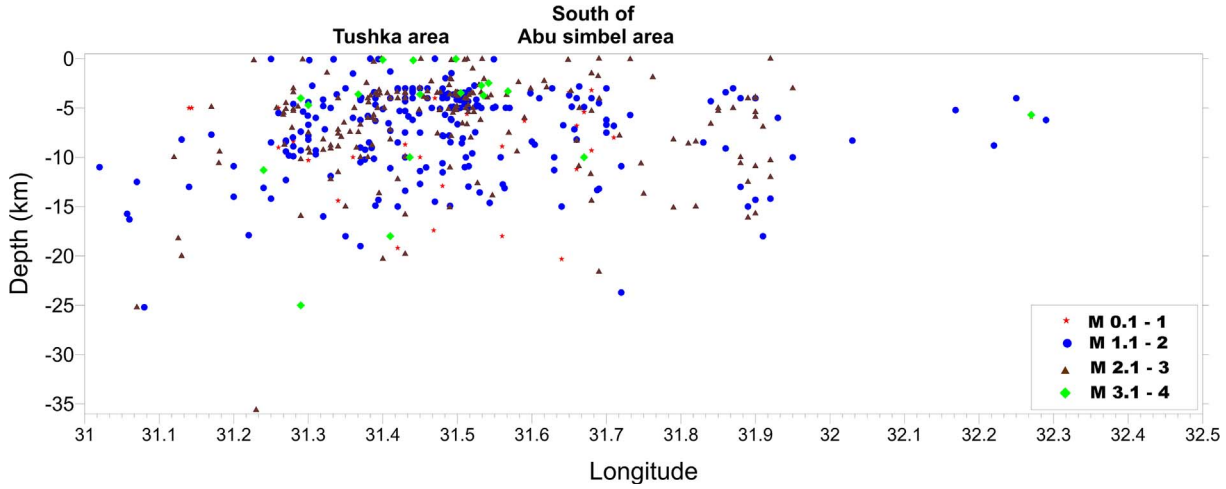

Fig. 5. Cross section shows distributions of earthquake events in west-east direction crossing Tushka New city area.

4.1. 2-D gravity modelling

To obtain a more quantitative representation of the subsurface structure in the study area, 2D density models were constructed along the N–S and E-W profiles (Fig. 7). The modelling method optimizes either the density or the height of the individual blocks so that the divergence between the measured and the computed gravity data gets minimized. The majority of the existing algorithms for modelling gravity data assume that the density above the basement interface is uniform, allowing the use of constant-density modelling schemes (Bhattacharyya and Navolio, 1975). To compute 2D density models, the density for different layers in the sedimentary section was taken as the average, i.e., 2.4 gm/cm^3, while for the basement layer it was set to 2.67 gm/cm^3. The forward model was made using polygonal bodies. The position, shape, dimensions, and density contrast were set to get the best fit between the observed and calculated data. The amplitude of

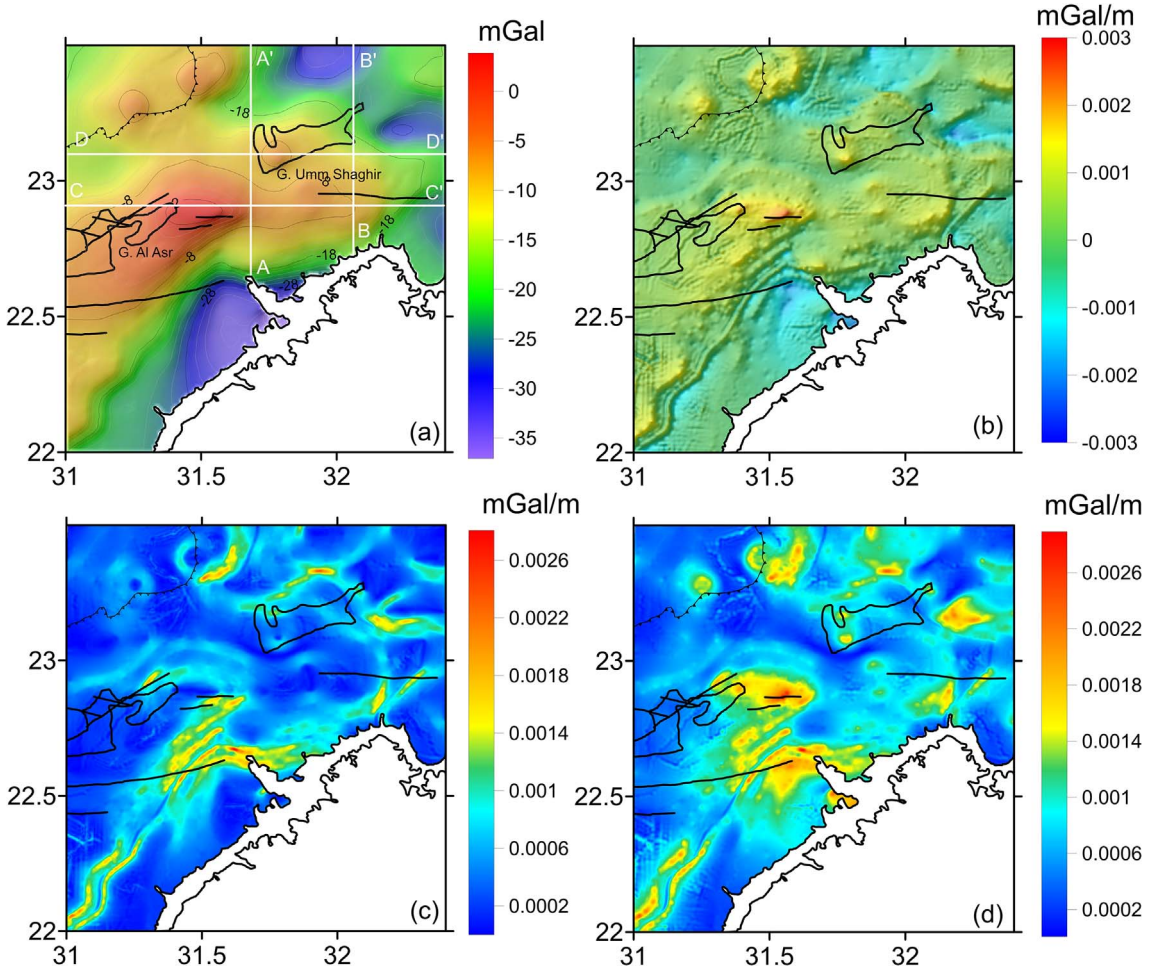

Fig. 6. (a) Bouger anomaly map of the study area compiled by the Egyptian General Petroleum Corporation [E.G.P.C.] (1980). The white lines refer to the locations of profiles using for 2D modeling, and its derivative maps; (b) the first vertical gradient, (c) a horizontal gradient, and (d) a tilt gradient.

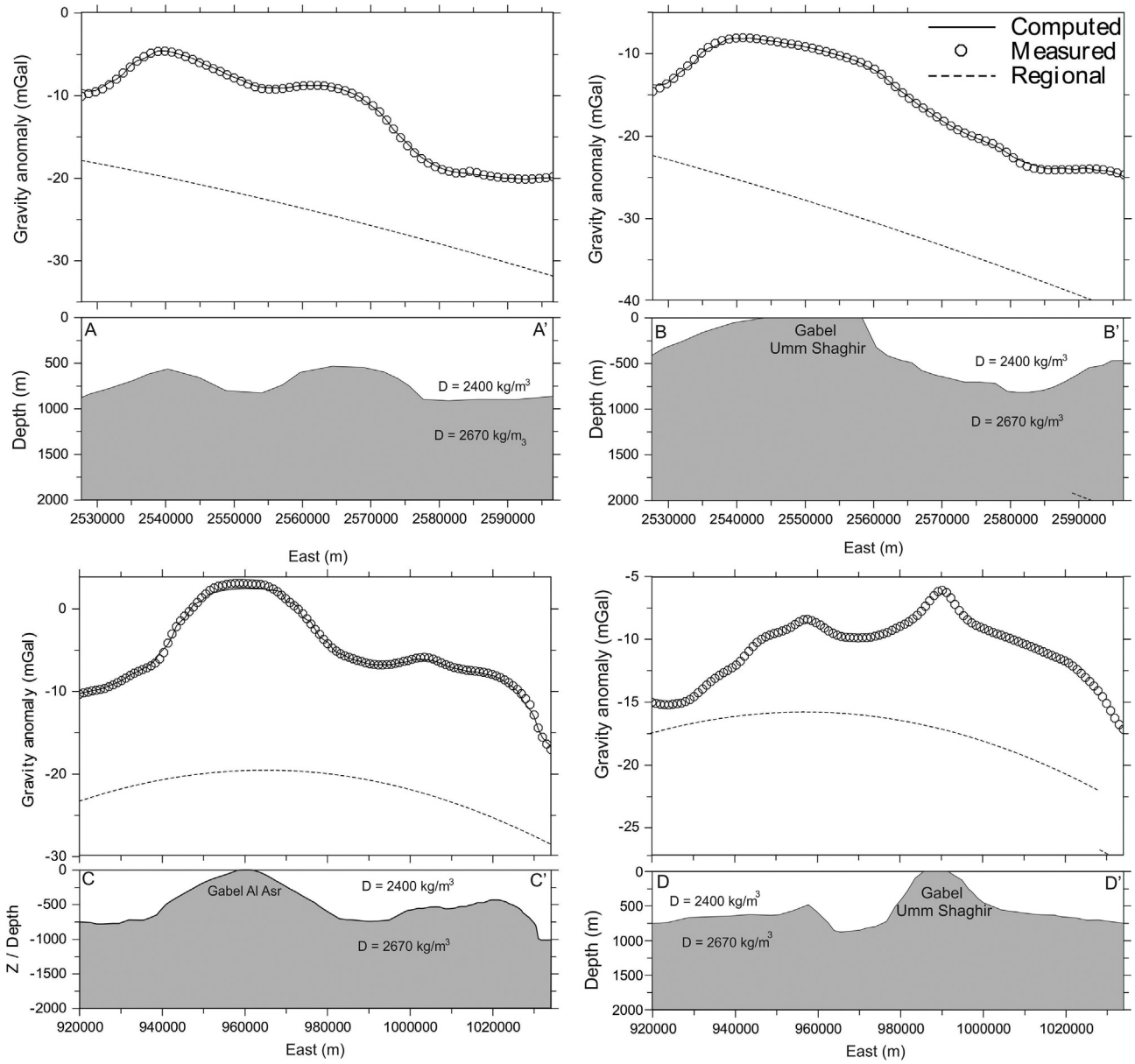

Fig. 7. Two-dimensional gravity models along four N–S and E-W profiles. Numbers in the cross-section denote model densities in kg/m^3 and the locations of these profiles are shown in Fig. 6a.

the gravity anomaly is proportional to the contrast between its density and the background density while the shape of an anomaly depends essentially on the size and shape of the related source structures. The gravity models were conducted along four profiles AA′, BB′, CC′ and DD′ (Fig. 7a–d consequently). The depth to basement rock increases eastward and northward (the greater depth is 700 m). Basement outcrops at Al Asrand Umm Shaghir areas were used as control points to verify the gravity modeling results.

5. Geoelectric measurements

Twenty-four vertical electrical soundings (VES's) are measured in the study area, along two profiles, A.A′ profile of NE-SW and B-B' of SE-NW (Fig. 1). The well Known Schlumberger configuration of electrode separation starting from AB/2 = 1.5 m up to AB/2 = 1000 m (maximum AB/2) is selected and applied. It is fortunate that, a numbers of boreholes (ofthe Research Institute for Groundwater RIGW) are selected near some measured VES's and are used for correlations between the interpreted electrical data and the truesubsurface geological as well as hydrology information. The geoelectrical cross-areas can demonstrate the actual geoelectrical picture of the subsurface conditions that prevail in the study area. Likewise, plot the thicknesses and electric resistivity values characterizing the acquired geoelectrical units. The geoelectrical section, when compared with the available geological data, can obtain the geological interpretation attaining behind the hydrogeological conditions of the study area. The geoelectrical cross-sections are assembled and arranged between the electrical sounding stations as well as the lithologic logs, which are distributed along the two profiles at separate locations and directions.

The cross section A-A′ in Fig. 8 is composed of four geoelectrical units as follows: The first geoelectrical unit is characterized by very high resistivity of 5896 ohm m (VES No. 6) and 11,520 ohm m. in the south west (VES No. 1) which corresponds to a surface sand and gravel. The thickness of this unit is varied from 7.7 m. (VES No. 7) to 46 m (VES No. 1). The second geoelectrical unit is manifested by a relatively high resistivity ranged between 940 ohm m. (VES No. 5) and 2200 ohm m. (VES No. 1) which corresponds to dry fine sand (unsaturated zone of Nubian sandstone). The thickness of this unit is varied from 33.8 m

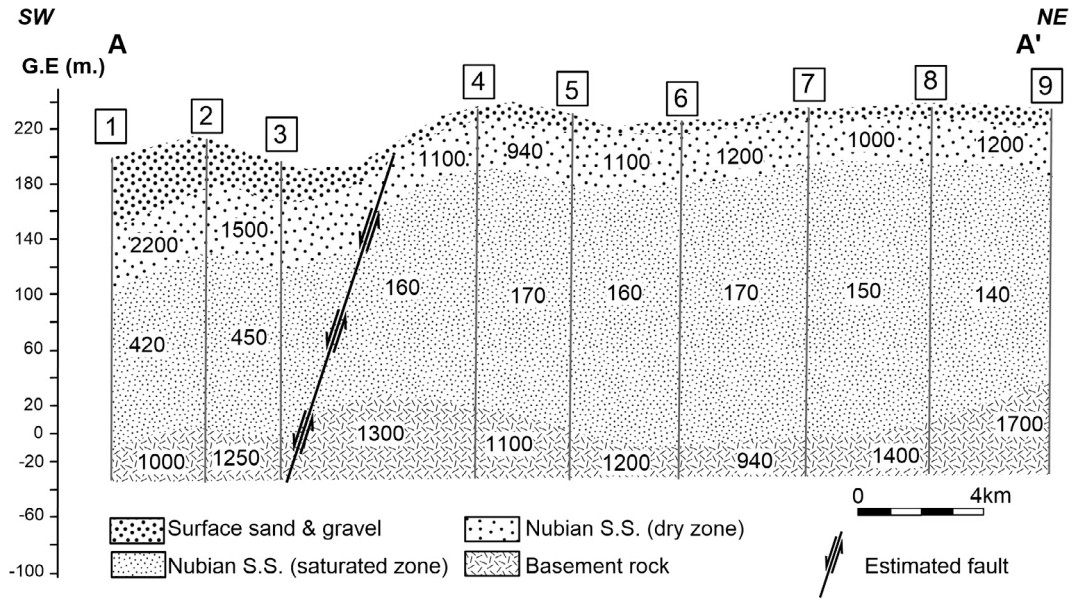

Fig. 8. Interpreted geoelectrical cross section along profile (A-A′), the numbers inside the cross section refer to apparent resistivites in ohm m. The location of the profile is shown in Fig. 1.

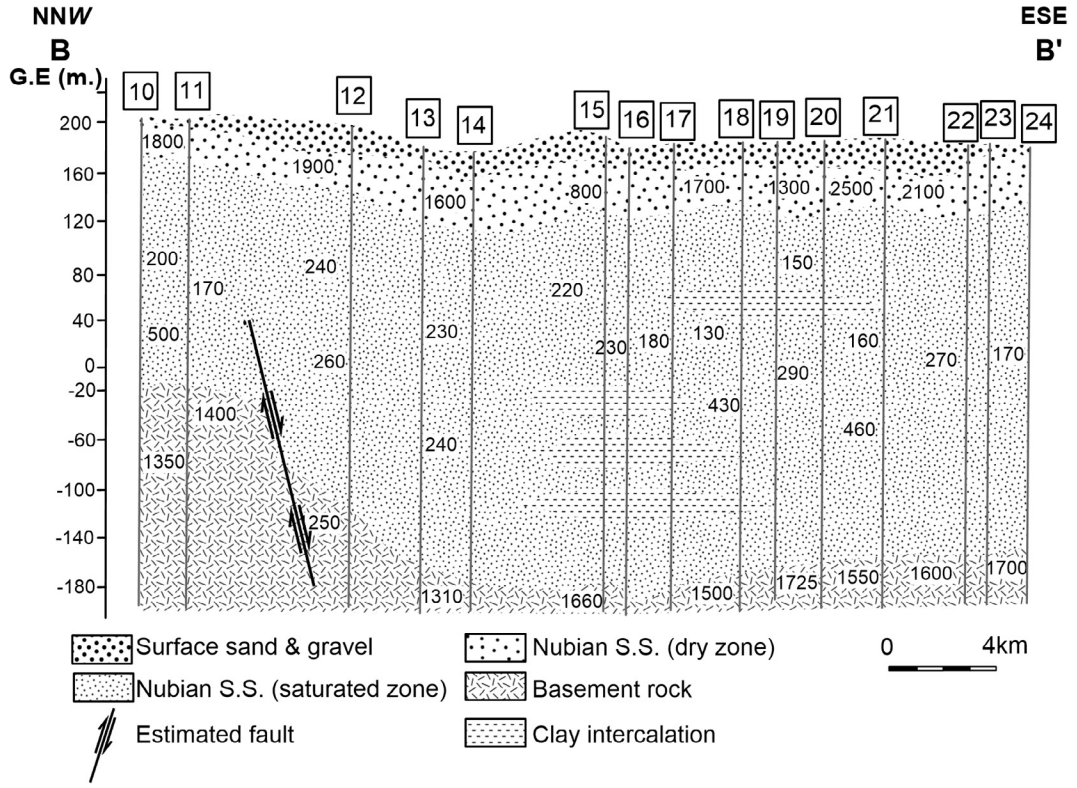

Fig. 9. Interpreted geoelectrical cross section along profile (B-B′), the numbers inside the cross section refer to apparent resistivites in ohm m. The location of the profile is shown in Fig. 1.

(VES No. 7) to about 46 m. (VES No. 2). The third geoelectrical unit is implied by a relatively medium resistivity varied from 140 ohm m. (VES No. 9) and 650 ohm m. (VES No. 2) which corresponds to coarse sandstone (Nubian aquifer in the study area). The thickness of this unit is varied from 114 m. (VES No. 1) to 194 m. (VES No. 7). The fourth geoelectrical unit is characterized by high resistivity which relates to basement rocks. The abrupt change in the values of electrical resistivity of the layers, which appears between (VES No. 4) and (VES No. 3) can be explained by an expected fault between them.

The geoelectrical cross–section B-B′ in Fig. 9 is constituted from by four geoelectrical units as follows: The first geoelectrical unit is characterized by a very high resistivity ranged between 236 ohm m. (VES No. 15) and 19,285 ohm m in (VES No. 22) which corresponds to a surface sand and gravels. The thickness of this unit ranges from 3.6 m. (VES No. 10) to 46 m. (VES No. 21). The second geoelectrical unit is manifested by a values relatively high resistivity values ranged between 800 ohm m. (VES No. 15) and 2500 ohm m. (VES's No. 20 and 21), Which corresponds to dry fine sand (unsaturated zone of Nubia Sandstone). The thickness of this unit is varied from 25 m (VES No. 10) to about 51 m (VES No. 14). The third geoelectrical unit is implied by a

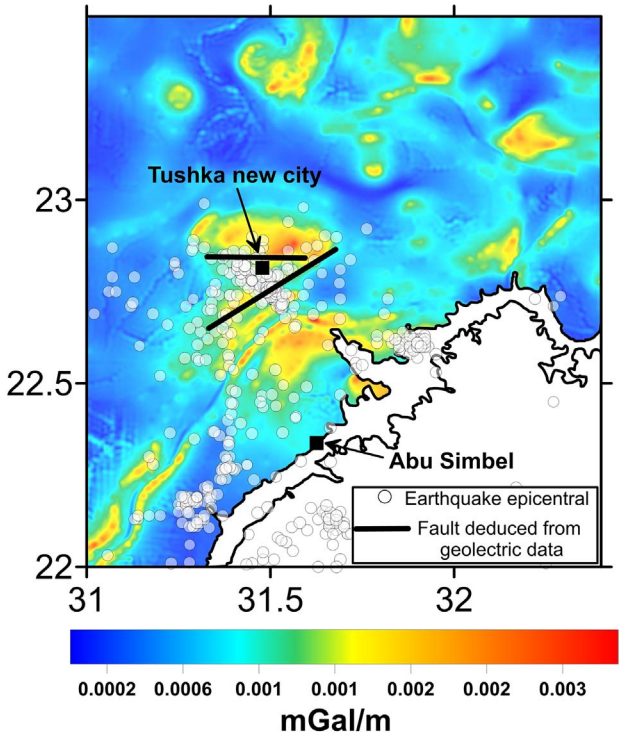

Fig. 10. An integrated map of analytical signal of Bouguer anomaly map, distribution of Earthquake epicentral and faults deduced from geoelectrical profiles.

relatively medium resistivity varied from 170 ohm m (VES No. 11) and 460 ohm m (VES No. 21), which corresponds to coarse sandstone with ground water which represents the main Nubia aquifer in the study area with clay intercalation. The thickness of this unit is varied from 200 m. (VES No. 10) to 311 m. (VES No. 15). The fourth geoelectrical unit is revealed by high resistivity values, which corresponds to basement rocks. The resistivity values range from 1300 ohm m (VES No. 13) to 1700 ohm m. (VES No. 24). The abrupt change in the values of electrical resistivity of the layers, which appears between (VES No. 11) and (VES No. 12) can be explained by an expected fault between them (see Fig. 10).

6. Results and conclusion

The geologic formation, regularly contains interconnected fractures/faults zones on a continuum of scales (Bonnet et al., 2001) caused by cooling and/or tectonic processes. Integrated geophysical tools (seismicity, gravity and geoelectric tools) were utilized for studying the tectonic structure in south west of the Lake Naser. The area of south of Abu Simbellies about 270 km to the southwest of Aswan has seismic activity and correlated with surface geology where showed some faults with different direction, N-S; E-W; NE-SW and NW-SE (El-Shazly and Abd El Hady, 1977). The seismic activity here was dispersed in various directions with extent up to 4.2. On the other hand, the seismic activity in Tushka zone, northwest of Abu-Simbel, can be considered as an expansion of Abu-Simbel occasions. The majority of the seismic events were found recently and characterized by magnitude running up to 2.8. This zone has an extraordinary significance from the developing perspective where the national Tushka venture is built.

The most significant features in the Bouguer anomaly map are the steep gradients from high to low gravity values at the northern margin of Lake Naser (NE-SW striking trend). The steep gradient can be interpreted as being associated with large normal and strike slip faults that control the structure of Lake Naser. This linear features with a NE-SW striking trend are pronounced in all processed gravity maps.

The geoelectrical cross-sections distinguished four geoelectrical units; The first unit is surface sand and gravel with very high resistivity, the second unit is correspond to dry fine sand (unsaturated zone of Nubian sandstone) which charcterizzed by a relatively high resistivity. The third unit is characterized by a relatively medium resistivity which corresponds to coarse sandstone (Nubian aquifer) while the end unit is correspond to basement rocks with very high resistivity values. The thickness of the main Nubia aquifer in the study area vary from 114 to 300 m.

This study shows the integration of the results from our geophysical studies using seismicity, gravity and geoelctric methods. It demonstrates a good coherence between the abundance of epicentral distributions of the recorded earthquakes, the existence of faults deduced from geoelctric measurements and the Linear features on the analytical signal of Bouguer anomaly map.

References

Bhattacharyya, B.K., Navolio, M.E., 1975. Digital convolution for computing gravity and magnetic anomalies due to arbitrary bodies. Geophysics 40 (6), 981–992.
Bonnet, E., Bour, O., Odling, N.E., Davy, P., Main, I., Cowie, P., Berkowitz, B., 2001. Scaling of fracture systems in geological media. Rev. Geophys. 39 (3), 347–383.
CONOCO Coral, and Egyptian General Petroleum Company, 1987. Geological map of Egypt, El Sad El Ali- and Bernise-sheets scale 1:500,000, Cairo, Egypt.
Cordell, L., Grauch, V.J.S., 1985. Mapping basement magnetization zones from aeromagnetic data in the San Juan Basin, New Mexico, in the utility of regional gravity and magnetic anomaly maps. Explor. Geophys, pp. 181–197.
Cordell, L., 1979. Gravimetric expression of graben faulting in Santa Fe Country and the Espanola Basin, New Mexico, in Guidebook to Santa Fe Country. In: 30th Field Conference, edited by R. V. Ingersoll, New Mexico Geological Survey, pp. 59–64.
Egyptian General Petroleum Corporation (EGPC), 1980. Bouguer anomaly map of South Western desert of Egypt, scale 1:500,000.
Grauch, V.J.S., 1987. A new variable-magnetization terrain correction method for aeromagnetic data. Geophysics 52, 94–107.
Khamis, M., Basheer, A., Rabeh, T., Khalil, A., EssamEldinA, A., Sato, M., 2014. Geophysical assessment of the hydraulic property of the fracture systems around Lake Nasser-Egypt: in sight of polarimetric borehole radar. NRIAG J. Astron. Geophys. 3 (1), 7–17.
El Shazly EM,Abd El Hady MA, 1977. Geology and Groundwater Conditions of Toshka basin area, Egypt: In llth International symposium on Remote sensing of Environment; Groundwater in arid areas in Egypt, pp. 25–29.
Taha, R., Bedair, S., Miranda, M., Carvalho, J., Khalil, A., 2009. Subsurface structures and hydrogeologic aquifers at the western side of lake nasser, Southwestern Desert, Egypt. J. Environ. Eng. Geophys. 14 (2), 87–95.